CELL CYCLE
2019, VOL. 18, NO. 4, 413–424
https://doi.org/10.1080/15384101.2019.1568745

Taylor & Francis
Taylor & Francis Group

RESEARCH PAPER

OPEN ACCESS Check for updates

ARPE-19-derived VEGF-containing exosomes promote neovascularization in HUVEC: the role of the melanocortin receptor 5

Rosa Maisto[a], María Oltra[b], Lorena Vidal-Gil[b], Natalia Martínez-Gil[c], Javier Sancho-Pellúz [b], Clara Di Filippo[a], Settimio Rossi[a], Michele D´Amico[a], Jorge Miguel Barcia [b], and Francisco Javier Romero [c]

[a]Department of Experimental Medicine, Università degli studi della Campania Luigi Vanvitelli, Napoli, Italy; [b]Neurobiología y Neurofisiología, Facultad de Medicina, Universidad Católica de Valencia "San Vicente Mártir", Valencia, Spain; [c]Department of Basic Medical Sciences, Universidad Europea de Valencia, Valencia, Spain

ABSTRACT

ARPE-19 retinal pigment epithelial cells cultured in a medium containing 35 mM D-glucose led to an augmented ROS formation and release of vascular endothelial factor (VEGF)-containing exosomes compared to ARPE-19 cells cultured in a medium containing 5 mM D-glucose (standard medium). Exposing these cells to the melanocortin 5 receptor agonist (MCR_5) PG-901 (10^{-10}M), for 9 d reduced ROS generation, the number of exosomes released and their VEGF content. In contrast, incubating the cells with the melanocortin receptor MCR_1 agonist BMS-470539 (10^{-5} M) or with the mixed $MCR_{3/4}$ agonist MTII (0.30 nmol) did not produce any significant decrease in ROS levels. ARPE-19-derived VEGF-containing exosomes promoted neovascularization in human umbilical vein endothelial cells (HUVEC), an effect that was markedly reduced by PG-901 (10^{-10}M) but not by the $MCR_{3/4}$ agonist MTII (0.30 nmol) or the MCR_1 agonist BMS-470539 (10^{-5} M). The MCR_5-related action in the ARPE-19 cells was accompanied by the increased expression of two coupled factors, cytochrome p4502E1 (CYP2E1) and nuclear factor kappa b (Nf-κB). These are both involved in high glucose signalling, in ROS generation and, interestingly, were reduced by the MCR_5 agonist in the ARPE-19 cells. Altogether, these data suggest that MCR_5 is a modulator of the responses stimulated by glucose in ARPE-19 cells, which might possibly be translated into a modulation of the retinal pigment epithelium response to diabetes in vivo.

ARTICLE HISTORY
Received 14 May 2018
Revised 7 December 2018
Accepted 12 December 2018

KEYWORDS
Diabetes; melanocortin receptors; oxidative stress; vasculogenesis; exosomes

Introduction

The melanocortins α-, β-, and γ-melanocyte-stimulating hormone (α-, β-, γ-MSH) and adrenocorticotropic hormone (ACTH) are a family of peptides that exert several biological activities, including pigmentation, steroidogenesis, energy homeostasis, exocrine secretion, sexual function, analgesia and the promotion of the resolution phase of inflammation through five distinct receptors, termed MCR_1, MCR_2, MCR_3, MCR_4, and MCR_5 [1]. These receptors are 7-transmembrane G protein-coupled receptors that are ubiquitously expressed in several organs, including the eye. MCR_3 and MCR_4 are localized in the layer of retinal ganglion cells, whilst the retinal pigment epithelial cells abundantly express MCR_5 [2]. Recent in vivo studies demonstrated that the activation of MCR_5 exerts anti-angiogenic activity, in the retina of diabetic mice [3,4]. However, there are no clear hints about the down-stream signaling of MCR_5 activation and related anti-angiogenic activity. Furthermore, no insights have been gained for identification of retinal cell type involved in the protective effect of MCR_5 agonists.

Recent clinical data have shown that high levels of circulating exosomes are detected in diabetic patients and participate in the transport of pro-angiogenic factors leading diabetic retinopathy [5]. Although these results pave the way for an exosomes-related mechanism in development of diabetic retinopathy, they do not address the cellular localization of exosome release and the retinal cellular targets of exosomes. A potential target of cytokines-releasing exosomes would be the retinal pigmented epithelium (RPE), which regulates retinal homeostasis, acting as a mediator between the choroid (vascular tunica) and the photoreceptor cell layer. Particularly, RPE is sensitive to oxidative stress induced by hyperglycaemia during diabetes [6]. Recent in vitro data from ARPE-19 human retinal pigment epithelial cells, indicate that

CONTACT Michele D´Amico michele.damico@unicampania.it

oxidative stress (OS) to these cells promotes the release of exosomes containing VEGF and VEGF receptors into the medium. These reactive oxygen species (ROS)-induced VEGF positive exosomes promote the development of new vessels when exposed to HUVEC [2]. Thus suggesting that an exosome-related neoangiogenesis may play a pivotal role in the pathology of retinal pigment epithelial cells in vivo, such as that observed in diabetic retinopathy, where OS and neoangiogenesis are important determinants.

Exosomes are small, 50 and 150 nm in diameter, cell-derived vesicles, that are released in several fluids, including blood, urine, and the medium of cell cultures [7,8]. Exosomes are released either by the cell, when multivesicular bodies fuse with the plasma membrane, or directly from the plasma membrane, under several stimuli [9]. Exosomes behave as paracrine effectors that influence the recipient cell, because they contain genetic material, proteins and factors essential for cell-cell communication [2], which can be transferred from one cell to another [10]. Moreover, exosome production and content may be influenced by molecular signals received from the cell of origin [11].

Based on these in vitro and in vivo evidences, we focused our study on the role of ARPE-19 derived VEGF-containing exosomes in neoangiogenesis, along with the activation of MCR_5, in order to shed ligh on the mechanism of action through which MCR_5 agonists inhibit angiogenesis in a in-vivo model of diabetic retinopathy, previously observed by Rossi et al. 2016. To test this hypothesis, we cultured HUVEC with exosomes released from high-glucose-stimulated ARPE-19 cells. The role of MCR_5 in exosome induced neoangiogenesis was tested by cell treatment with agonists targeting MCR_1, MCR_5, MCR_3 and MCR_4 receptors.

Results

Expression of the MCR receptors in ARPE-19 cells

Figure 1 shows that the ARPE-19 cells exposed to 35 mM D-glucose expressed non-significant higher levels of MCR_{1-4}, with respect to the cells exposed to 5 mM D-glucose. Whilst MCR_5 levels were significantly higher in the cells exposed to 35 mM D-glucose than those exposed to 5 mM D-glucose.

ARPE-19 cells increase ROS production under pro-oxidant challenges and effect attenuated by the MCR_5 agonist

Control ARPE-19 cells did not produce significant ROS levels, addition of 35 mM D-glucose (HG)

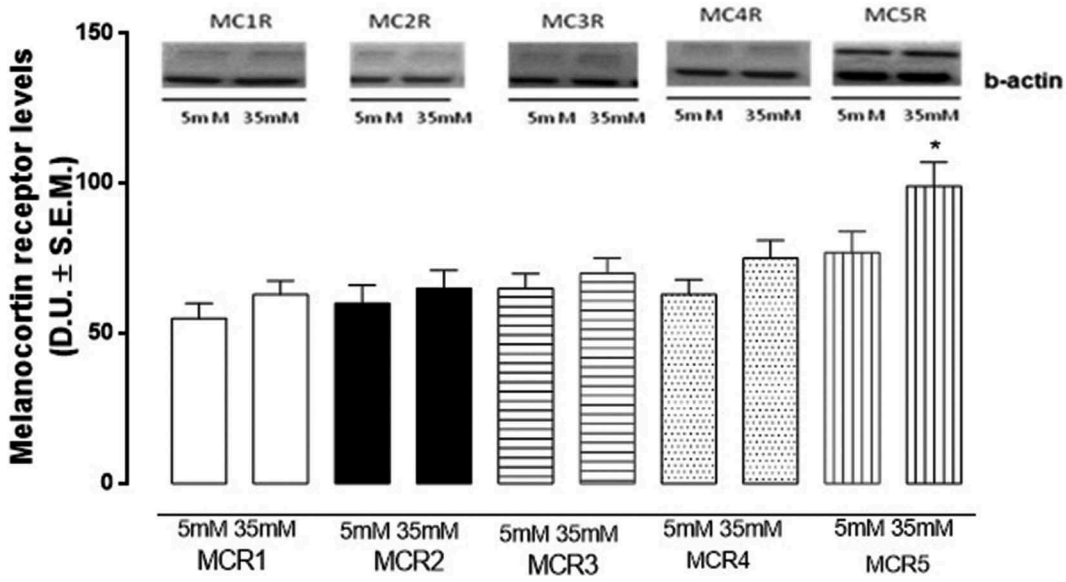

Figure 1. Melanocortin receptor protein expression. Western blot analysis showing the expression of the MCR subtypes in the ARPE-19 cells cultured in high-glucose conditions (HG, D-glucose, 35 mM) and standard medium control (CNT, 5 mM glucose). The values are expressed as the mean ± S.E.M. The experiments were repeated three times to ensure the consistency of the results. Significance levels are expressed as $P < 0.01$ (*) *versus* MCR_5 (5 mM glucose). D.U. = Densitometric Units.

resulted in a significant increase in ROS production. In the presence of the MCR_5 agonist PG-901 (10^{-10}M), this increase was significantly reduced. To determine if this effect was limited to MCR_5 activation, cells were incubated with the melanocortin receptor MCR_1 agonist BMS-470539 (10^{-5} M) or with the mixed $MCR_{3/4}$ agonist MTII (0.30 nmol), neither compound displayed a significant decrease in ROS levels ($P < 0.01$) (Figure 2), thus excluding the active participation of these receptors in the ARPE-glucose-ROS circuit.

PG-901 treatment increases the ARPE-19 cell survival following high glucose exposure

The XTT assay was then utilized to determine cell viability, treatment of ARPE-19 cells with the 35 mM D-glucose medium significantly reduced cell viability compared to the standard medium (CNT) ($P < 0.05$ *vs* CNT). ARPE-19 cells exposed to HG and incubated with PG-901 (10^{-10}M) for 24 hours showed a significant increase in survival compared to cells exposed to high glucose alone ($P < 0.01$ vs HG), indicating a positive interference with mitochondrial activity (Figure 3).

Oxidative challenges increase VEGF exosomes release and effect attenuated by the MCR5 agonist

Nine days after HG or H_2O_2 exposure, ARPE-19 cells released extracellular vesicles (Figure 4), as measured with the NanoSight technique. The extracellular medium containing 35 mM D-glucose resulted in an 80% significant increase in the level of the exosomes labelled for VEGFR2 (CD9-VEGFR2) (Figure 5) and for VEGF (CD9-VEGF) (Figure 6), with respect to the medium containing 5 mM D-glucose. In accordance with the previous finding, the addition of 10^{-10}M PG-901 (MCR5 agonist) reduced the number of CD9-VEGFR2 and CD9-VEGF exosomes (Figures 5 and 6).

ELISA and western blot analyzes indicated that VEGF, ANX2 and flotillin-1 protein levels were increased after pro-oxidant challenges with both HG and H_2O_2 and were reduced by PG-901 (MCR_5 agonist) in ARPE-19 cell homogenates and in the exosomes released from them (Figure 7(a-d)).

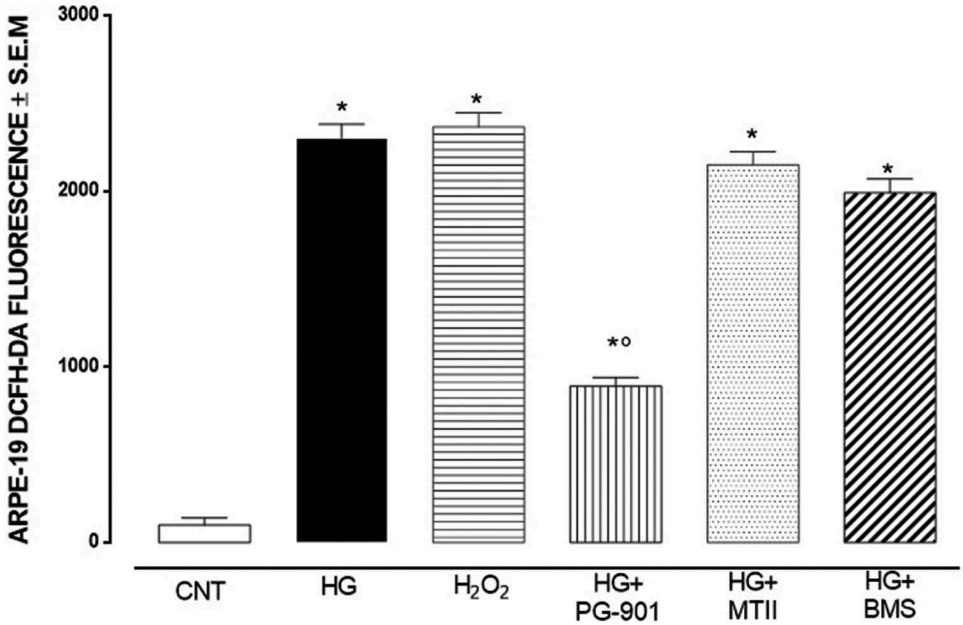

Figure 2. ARPE-19 ROS production. Total intracellular ROS from the ARPE-19 cells exposed to: standard medium (CNT 5 mM glucose); High Glucose (HG, 35 m^M); H_2O_2 (100 μM); HG+PG-901 (10^{-10}M); HG+MTII (0.30 nmol); HG+BMS-470,539 (10^{-5}M) analyzed by H2DCFH. The values are expressed as the mean ± S.E.M. The experiments were repeated three times to ensure the consistency of the results. The significance levels are expressed as $P < 0.01$ (*) *versus* CNT, $P < 0.01$ (°) *versus* HG.

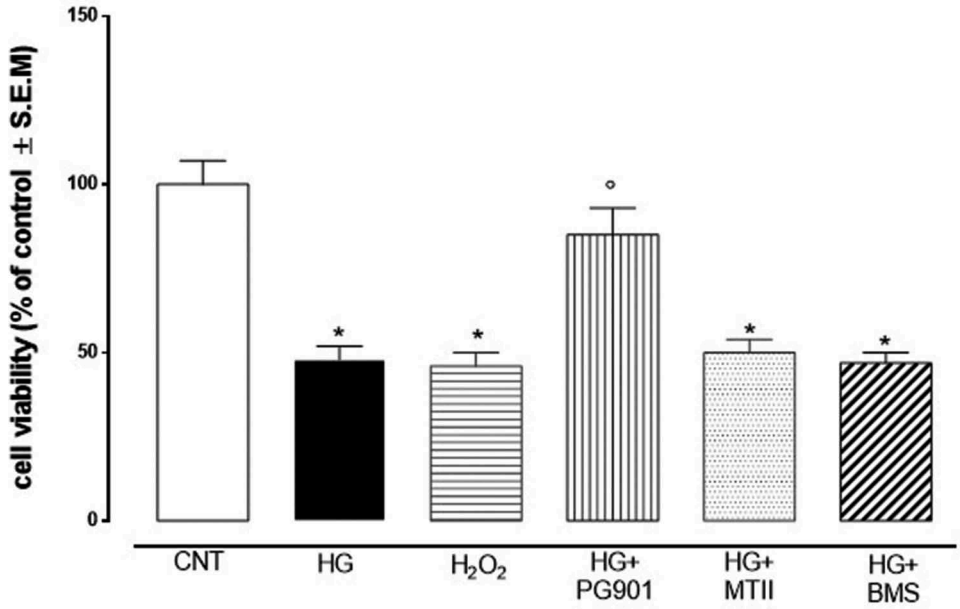

Figure 3. XTT assay showing the cell viability as a percentage of the standard medium (CNT). Compared to the CNT, 35 mM glucose (HG) led to a significant decrease of the cell viability. PG-901 (10^{-10}M) increased cell survival in the ARPE-19 cells exposed to 35 mM glucose. Cell viability after the HG+MTII ($MCR_{3/4}$ agonist, 0.30 nmol) and H_2O_2+ MTII; HG+BMS (MCR_1 agonist, 10^{-5}M) treatments. The results are reported as the mean ± S.E.M. The experiments were repeated three times to ensure the consistency of the results. $P < 0.01$ (*) *versus* CNT; $P < 0.01$ (°) *versus* HG.

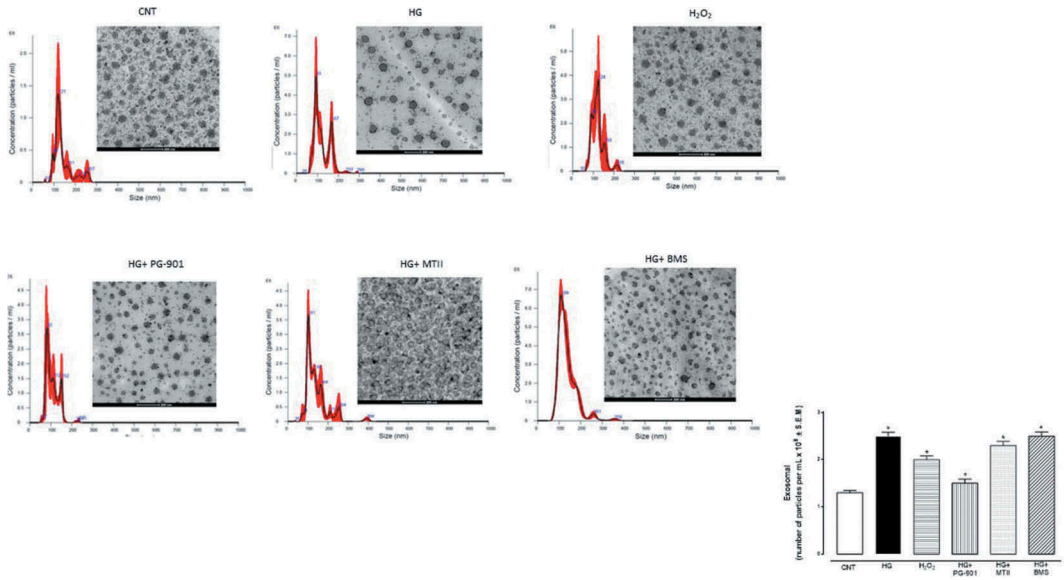

Figure 4. C**haracterization of the exosomal vesicles released by the treated or untreated ARPE-19 cells**. Size-distribution of exosomes assessed using a Nanoparticle Tracking Analysis, and their release into the extracellular medium assessed by electron microscopy. Scale bar 200 nm. The experiments were repeated three times to ensure the consistency of the results. The significance levels are expressed as $P < 0.01$ (*) *versus* control (CNT) and $P < 0.01$ (°) *versus* HG. CNT = standard medium; HG = 35 mM D-glucose.

ARPE-19 released exosomes promote vasculogenesis

In the absence of exosomes, HUVEC produce little vascular processes. Similarly, exosomes derived from vehicle (control)-treated ARPE-19 cells promoted few nodes and tubes (Figure 8). In contrast, the HG- (35 mM) and H_2O_2- (100 μM) induced exosomes resulted in a significant increase in HUVEC tube

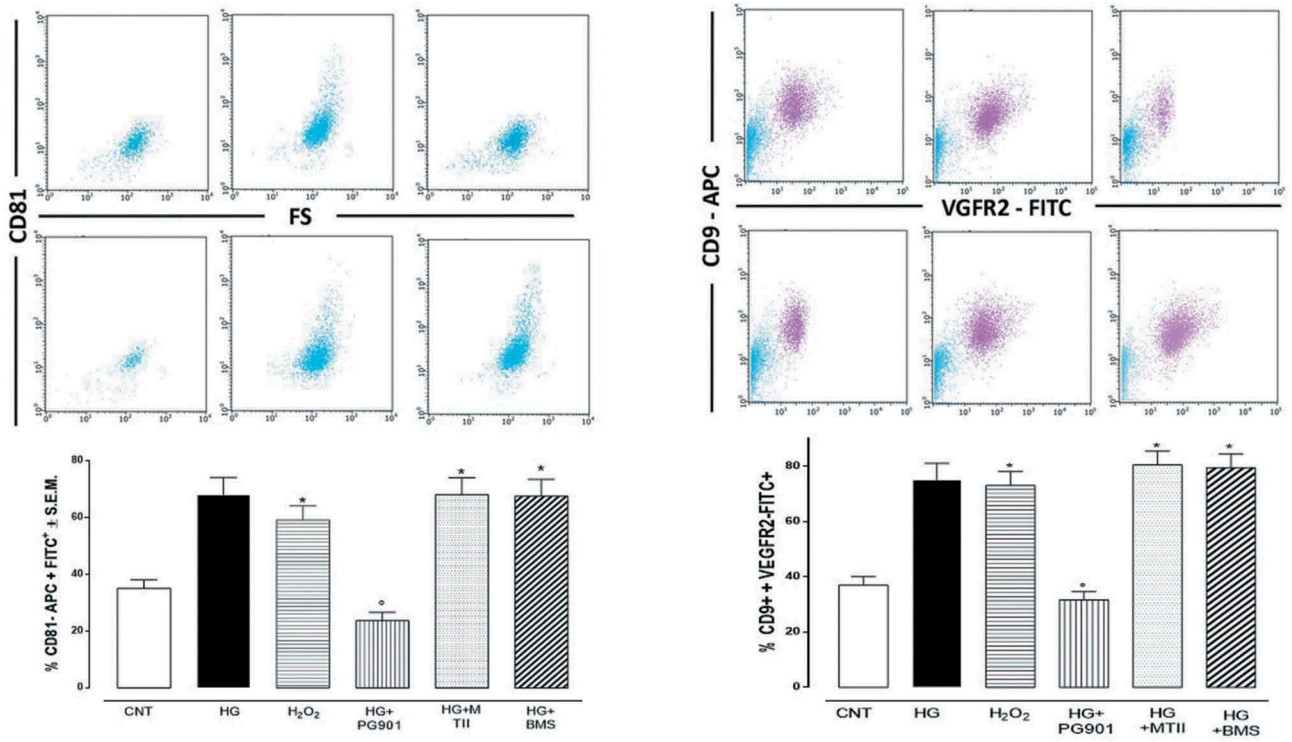

Figure 5. Characterization of the exosomal cargo. The ARPE-19-released exosomes were isolated and were scrutinized by flow cytometry, targeting anti CD9-VEGFR2 and CD-81, with the relative quantification expressed in the bar graph. The experiments were repeated three times to ensure the consistency of the results. The significance levels are expressed as $P < 0.01$ (*) *versus* control (CNT) and $P < 0.01$ (°) *versus* HG. CNT = standard medium; HG = 35 mM D-glucose.

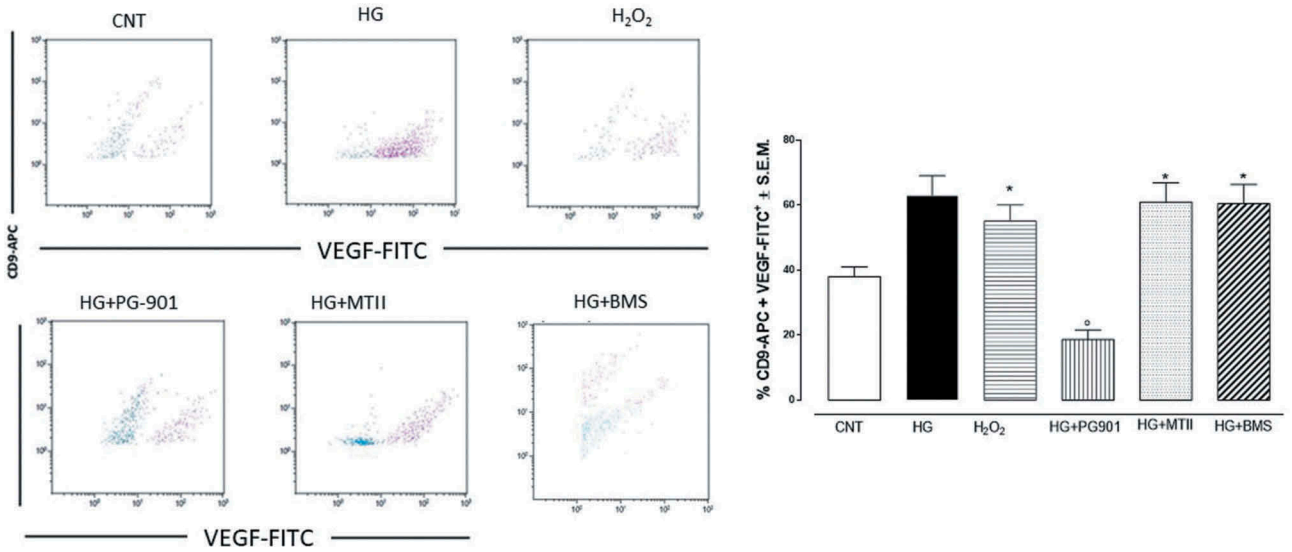

Figure 6. ARPE-19-released exosomes by flow cytometry, targeting anti CD9-VEGF. The treatments were as shown in Figure 5, and were repeated three times to ensure the consistency of the results. The significance levels are expressed as $P < 0.01$ (*) *versus* control (CNT) and $P < 0.01$ (°) *versus* HG. CNT = standard medium; HG = 35 mM D-glucose.

formation, with a significant increase in nodes and tubes. In particular, comparing EXO (CNT) to CNT, the vascular morphology, the mean node formation and the mean tube formation were changed as consequence of the augmented VEGF bioavailability within the exosomes. Interestingly, the exosomes induced from the HG+MCR_5 agonist PG-901-treated cells resulted in a significant decrease in tube

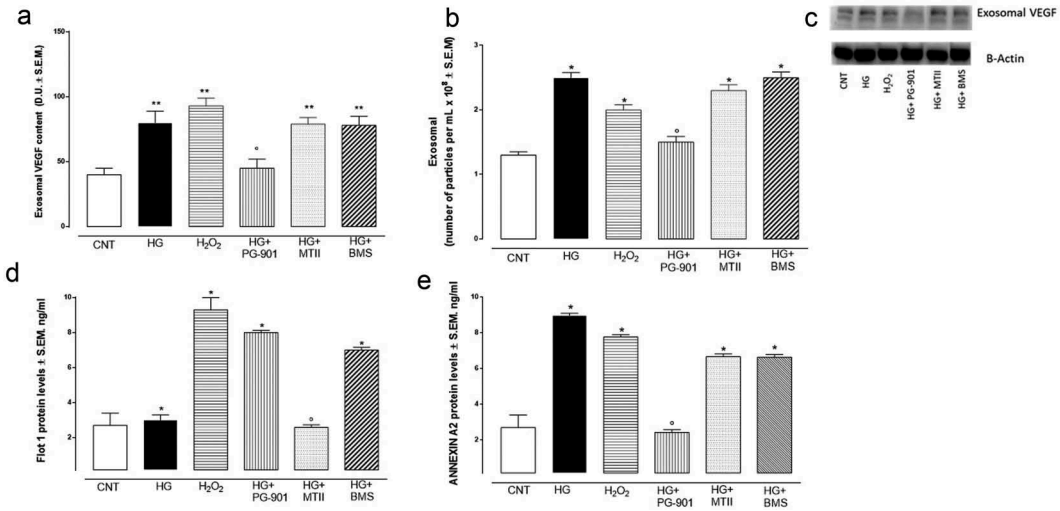

Figure 7. VEGF expression in the ARPE-19 cells and ARPE-19-isolated exosomes. (a) The VEGFA protein levels were measured by an ELISA assay in the ARPE-19 cells. (b, c) The VEGF protein levels were measured by a western blot in the exosomes. (d) Flotillin-1 levels. (e) ANXA2 levels. The experiments were repeated three times to ensure the consistency of the results. The values are expressed as (pg/ml) the mean ± S.E.M. (N = 3 repeats). The significance levels are expressed as $P < 0.05$ (*) *versus* CNT, $P < 0.01$ (**) *versus* CNT $P < 0.01$ (°) *versus* HG. CNT = standard medium; HG = 35 mM D-glucose; D.U. = Densitometric Units.

and node formation (Figure 8). In contrast, the $MCR_{3/4}$ agonist MTII (0.30 nmol) or the MCR_1 agonist BMS-470539 (10^{-5} M) did not affect vasculogenesis (Figure 8).

Oxidative-induced NF-κB and Cyp2E1 expression are modulated by the MCR_5 agonist

Western blot analysis indicated (Figure 9) that both pro-oxidant challenges (HG and H_2O_2) led to

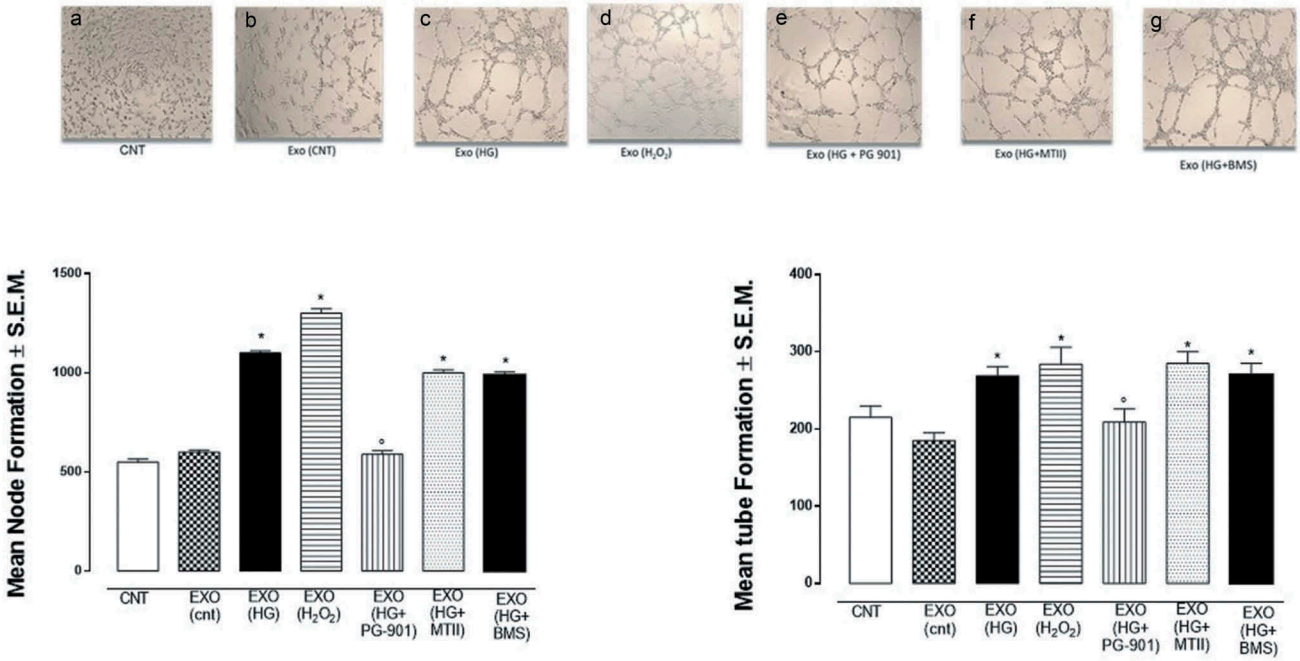

Figure 8. Exosome-induced Vasculogenesis in HUVEC. Representative images of the tubular structures from: (a) HUVEC seeded with exosome-free medium; (b) HUVEC seeded with exosome-containing medium; (c) HUVEC seeded with HG- (35 mM) induced exosomes; (d) HUVEC seeded with H_2O_2- (100 µM) induced exosomes; (e) HUVEC seeded with the HG+MCR_5 agonist PG-901 (10^{-10}M); (f) HG+$MCR_3/_4$ agonist MTII 0.30 nmol; (g) HG+BMS (10^{-5}M); (h) Node formation and (i) Tube formation. Scale bar 500 µm. The experiments were repeated three times to ensure the consistency of the results. The values are expressed as the mean ± SEM. The significance levels are expressed as P < 0.01 (*) *versus* EXO (CNT) and P < 0.01 (°) *versus* HG. CNT = ARPE-19 cells in standard exosome free medium.

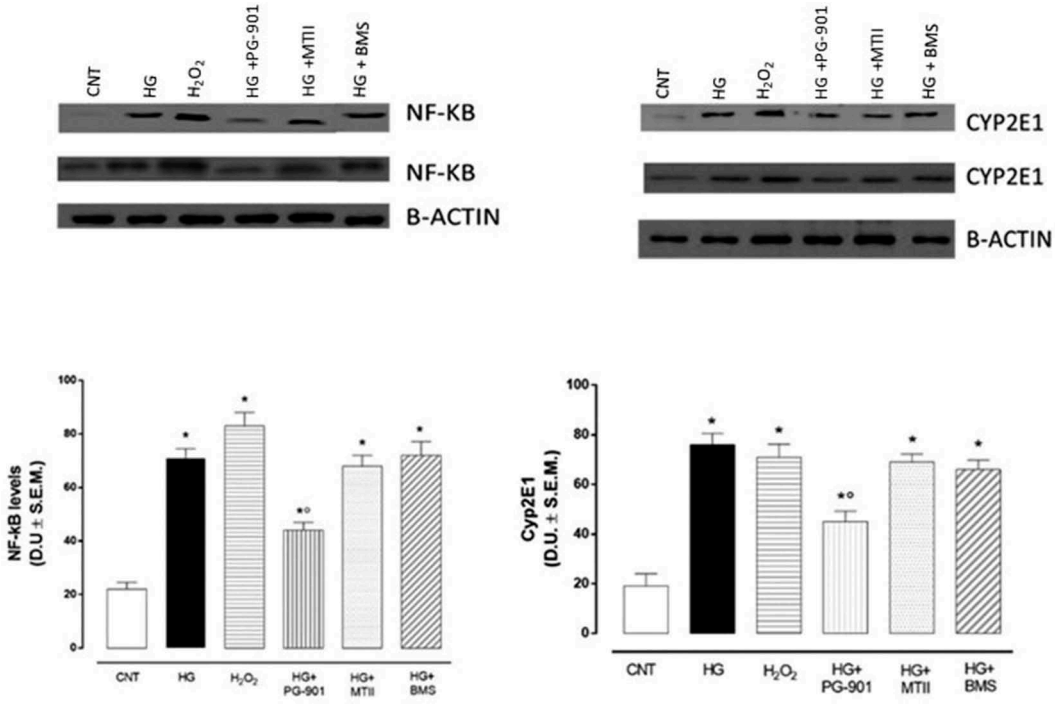

Figure 9. NF-kB and Cyp2E1 protein expression. Representative images of NF-kB and Cyp2E1 and relative levels assessed by the densitometry of the bands at 65 kD (NF-kB) and 57 kDa (Cyp2E1) are presented. β-Actin was used as the loading control. The data are expressed as densitometric units (D.U.) and are presented as the mean ± S.E.M. The experiments were repeated three times to ensure the consistency of the results. The significance levels are expressed as $P < 0.01$ (*) *versus* control and $P < 0.01$ (°) *versus* HG.

a significant change in NF-κB and Cyp2E1 protein expression compared to control levels, this increase reduced in the presence of PG-901.

Discussion

One critical factor in diabetes is the glucose over drive that finally results in ROS production [12,13] and pro-inflammatory markers, affecting the cell membranes and proteins, leading to cell dysfunction or even cell death [14,15]. ROS is detrimental for cells in several organs, including the eye, where it alters the structure and functionality of retinal cells [16]. The latter includes amacrine cells, Müller cells, ganglion cells and the photoreceptors [4]. Within retinal cell types, the retinal pigmented epithelial (RPE) cell layer has a central role in maintenance of retinal homeostasis, providing nutrients from choroid to photoreceptor layer. RPE cells are sensitive to various oxidant injury stimuli, such as those induced by RPE exposure to visible light or those derived from endogenous metabolism [17–19]. Following these stimuli, RPE cells increase ROS and inflammatory mediators production and release, that influence the integrity and the function of the RPE itself and of other cells and tissues in the retina [20]. In this context, the present study showed that when ARPE-19 human retinal pigment epithelial cells were exposed to high glucose levels (35 mM), a condition that mimics the diabetic hyperglycaemia in vivo [4], a high-glucose driven overexpression of ROS was generated affecting in turn the survival of the cells themselves.

A consequence of the glucose-induced ROS overproduction in the eye is often the initiation of a process of vascular alterations, blood retinal barrier damage or leakage and cell proliferation [3]; leading then to retinal neovascularization [21,22]. This neovascularization is promoted by vascular endothelial growth factor (VEGF), fibroblast growth factor (FGF), tumour necrosis factor-alpha (TNF-α), transforming growth factor-beta (TGF-β), and angiopoietins [22]. Previous studies hypothesized that retinal neovascularization is triggered by a ROS-dependent release of VEGF-

containing exosome vesicles from the retinal cells, leading to the formation of the new vessels [2,22,23]. These exosomes are small vesicles, between 50 and 150 nm in diameter [2], which are released by several cell types and under different stimuli [24–28]. Exosomes contain genetic material, proteins and inflammatory factors essentials for cell-cell communication [2]. In our studies, high glucose concentration (35 nM) represented a strong stimulus to sustained ROS production and exosome release by the ARPE-19 cells, after nine days of exposure. These high glucose-induced exosomes were characterized by high VEGF content, which explains the angiogenic potential of high-glucose induced exosomes. Indeed, the exosomes increased node and tube formation in HUVEC cells, when derived from ARPE-19 cells cultured in high glucose medium. We described for the first time that ARPE-19 cells, challenged with high glucose levels (35 nM), release VEGF-containing exosomes capable to promote neovascularization in HUVEC cells.

Furthermore, we demonstrated that MCR_5 activation reverse the angiogenic potential of high glucose-induced exosomes, released by ARPE-19. In fact, the exosomal release from these cells and the consequent exosomes-induced node and tube formation in the HUVEC were significantly reduced by ARPE-19 treatment with PG-901, a melanocortin receptor MCR_5 agonist. The MCR_5 receptor plays a role in glucose metabolism- and inflammation-based pathologies [29,30], and is expressed in retinal pigment epithelial cells [4]. Human studies showed that single-nucleotide polymorphism in the MCR_5 was associated with type 2 diabetes in obese subjects, while experimental in vivo and ex vivo studies demonstated that a glucose uptake in skeletal muscles driven by α-MSH is markedly reduced in MCR_5 KO mice. Additionally, the specific blockade of MCR_5 with selective antagonists results in hyperglycemia during a glucose tolerance test in mice [29]. On another note, activation of MCR5 by α-MSH reduces the adipose tissue inflammation [30]. Moreover, MCR_5 activation reduced the insurgence of diabetic retinopathy in a murine animal model in vivo and photoreceptors damage in murine primary retinal cells [3,4]. In these previous studies, however, a primary role in angiogenesis inhibition was indicated for the MCR_1. This evidence was not confirmed in the in-vitro study herein presented, possibly due to a different expression profile of melanocortin receptors in murine photoreceptor and human ARPE-19 cells. Thus, we hypothesized that MCR_5 plays a major role in the antioxidative and defensive response to high glucose damage, at least at the RPE layer.

The role of MCR_5 is not limited, however, to the targets mentioned above. Indeed, the data herein presented report that the reduced angiogenic potential of exosomes released by ARPE 19 treated with a MCR_5 agonist was accompanied by the reduced expression of two coupled factors the cytochrome p4502E1 (CYP2E1) and nuclear factor kappa b (NF-κB), accordingly to previous evidences [31]. Both CYP2E1 and NF-κB are involved in response induced by high glucose and the ROS generation. Noteworthy, the activation of NF-κB by high glucose was demonstrated in several in vivo and in vitro studies [31], and the subsequent increase of CyP2E1 was related to the activity of this transcription factor [29]. Furthermore, CyP2E1 has been found to modulate oxidative stress and exosomes release in ARPE-19 cells [2]. To our knowledge, we hereby described for the first time, that activation of MCR_5 protects cells from the high glucose damage by modulation of the NF-kB and CyP2E1 pathways and therefore it deserves further investigation pertaining the impact of MCR_5 on CyP2E1 and NF-kB.

In conclusion, we demonstrated that the anti-angiogenic activity of MCR_5 agonists is related to modulation of exosomal release of VEGF by RPE cells, indicating that MCR_5 agonists can be developed as indirect inhibitors of angiogenesis. On the basis of evidences herein presented, other melanocortin receptors do not influence the exosome angiogenic potentials. In order to confirm in an in-vivo model the proposed mechanism of action of MCR_5 agonists, as indirect inhibitors of angiogenesis, we will treat non-diabetic mice with VEGF labelled exosomes isolated from primary retinal cells of diabetic mice, stimulated or unstimulated with MCR agonists. The angiogenic potential of exosomes will be evaluated in vivo by fluorangiography. Another interesting direction in further works would be showing the mechanism by which HG-induced OS causes the overexpression of MCR_5.

Material and methods

Cell culture

The retinal pigment epithelium (ARPE-19) human cell line was obtained from the American Type Culture Collection (ATCC). ARPE-19 cells and HUVEC isolated from umbilical veins as previously described [21] were cultured in Dulbecco's modified Eagle's medium/nutrient mixture F12 (DMEM/F12, Aurogene AU-L0093), glucose 5 mM (Life Technologies A4940-01), supplemented with Hepes 5 mM (Thermo Fisher 15630080), 7.5% NaHCO3 (Thermo Fischer 25080094), 10% inactivated foetal bovine serum (Thermo Fisher 10270106) and 1% penicillin/streptomycin (Aurogene Au-l0022) and maintained at 37°C and 5% CO2. Cells were used from passages 18 to 20 and cultured at a seeding density of 1×10^6 cells/cm^3 and experiments repeated three times. Two days after seeding, the culture media was exchanged and supplemented with 1% FBS instead of 10%. Cells were then split as follows, either incubated for 9 d with a high-glucose concentration at 35 mM (HG) or incubated for 24 hours with H_2O_2 (100 µM) as a positive control. Following this stimulation period, cells were treated for 24 hours with the MCR_5 agonist and $MCR_{3/4}$ antagonist PG-901 (10^{-10}M) [32,33], MCR_1 agonist BMS (BMS-470539, 10^{-5} M) [4], or with the mixed $MCR_{3/4}$ agonist MTII (0.30 nmol) [21], at concentrations previously reported in retinal cell cultures [4]. Subsequently, the cells and supernatants were collected and preserved for down stream analysis.

Western blot

ARPE-19 cells were collected in RIPA Buffer (Sigma-Aldrich R0278) and protease inhibitor cocktail (Roche 11873580001). Equal amounts of protein (20 µg) were loaded and analyzed by SDS-PAGE on 4–12% SDS-Polyacrylamide gel electrophoresis, and the proteins electroblotted onto polyvinylidene difluoride membranes (PVDF; Millipore IPFL10100) by wet transfer. Membranes were incubated overnight at 4°C with antibodies against MCR_1 (Abcam ab180776), MCR_2 (Abcam ab180793), MCR_3 (Abcam ab203671), MCR_4 (Abcam ab24233), MCR_5 (Abcam ab133656), VEGF (Santa Cruz Biotechnology sc-57496), NF-kB (Abcam ab32536), Cyp2E1 (Abcam, ab28146) and β-actin (Santa Cruz Biotechnology sc-8432), which was the loading control. Finally, the membranes were incubated for 2 hours at room temperature with anti-mouse (Santa Cruz Biotechnology sc-2005) or anti-rabbit IgG-HRP antibodies (Santa Cruz Biotechnology sc-2004). The bands were visualized with ECL (Pierce, Thermo Scientific, 32132) and detected with Image Quant LAS-400 mini (GE Healthcare, Uppsala, Sweden). Protein levels were quantified by densitometry using ImageJ software (NIH, Bethesda, MD, USA).

XTT assay

Cell viability, as measured by metabolic activity, was measured using 3′-[1- phenylaminocarbonyl-3,4-tetrazolium]-bis(4-methoxy-6-nitro) benzene sulfonic acid hydrate, (XTT, Cell Proliferation Kit II; Roche 11465015001). RPE cells were seeded at 6×10^3 cell/well in a 96-well cell culture plate for 24 hours. Cells were rinsed with PBS (Aurogene AU-L0615) twice and then were incubated with 0.3 mg/ml of the XTT final solution for 6 hours at 37°C in 5% CO_2. Metabolic activity was measured by a fluorescence multiple reader (Victor X5; Perkin Elmer) at 550 nm.

Determination of the ROS levels

ROS levels were measured using 2'7'-dichlorodihydrofluorescein diacetate (H2DCFDA; Santa Cruz Biotechnology CAS 4091–99-0), which is converted to a nonfluorescent derivate (H_2DCF) by intracellular esterases. This molecule is oxidized by ROS producing intracellular dichlorofluorescein (DCF). ARPE-19 cells were seeded at 6 × 103 cells/well in a 96 well plate and rinsed with PBS twice prior to incubation with 15 µM H_2DCFDA for 15 min at 37°C in 5% CO2. Total intracellular ROS production was measured by a fluorescence multiple reader (Victor X5; Perkin Elmer) at an excitation of 485 nm and an emission of 530 nm.

Exosomes isolation and size distribution

To determine exosome isolation, ARPE-19 cells were cultured as previously described using 1% Exosome-depleted FBS (Thermo Fisher 4478359). After 9 d, 10 mL of the culture media from the

treated and non-treated ARPE-19 cells were processed using the Total Exosomes Isolation Reagent from cell culture media (Thermo Fisher, 4478359) for exosomes isolation and resulting exosome pellet stored at 4°C in PBS 1x. Exosome identity was confirmed by nanoparticle tracking using the System NanoSight NS300 following the manufacture's protocol (Malvern Instruments, Malvern, UK).

Enzyme–linked immunosorbent assay (ELISA)

Quantitative determination of human vascular endothelial growth factor (VEGF) was assessed using a Human VEGF-A ELISA Kit (Abcam ab100662), Flotillin-1 (Biocompare, OKEH05627) and annexin A2 (ANXA2) (Antibodies online, ABIN415105) according to the manufacturer's instructions.

Electron microscopy

Exosome pellets were resuspended in PBS and were ultracentrifuged at 120,000 x g for 70 min at 4°C, approximately 10 μg of the samples were then resuspended in PBS on parafilm. The sample was fixed by depositing a drop of 2% paraformaldehyde (PFA) on the parafilm and placing the grid (Mesh with Formvar) on top of the drop. Negative staining was performed with 2% uranyl acetate. Photomicrographs were obtained using the FEI Tecnai G2 Spirit transmission electron microscope (FEI Europe, Eindhoven, Netherlands), with a Morada digital camera (Olympus Soft Image Solutions GmbH, Münster, Germany) and exosomes identified under the microscope (2000X magnification) solely based on size and morphology.

Flow cytometry

Exosomes were incubated for 1 hour at 4°C in rotation with anti-CD9-APC (Immunostep, Spain (anti-human CD45RA-clone HI100-Immunostep), a well-established exosome marker and Anti-CD81 (Thermo Fisher, MA, USA) antibodies. Exosomes were then incubated for 1 hour with anti-VEGF (Abcam ab10972) and for 30 min with FITC (Immunostep $9FEx_0$ −25). FACS Verse (Becton Dikinson, San Jose, CA, USA) was used to assess the exosomes, and 1,500,000 events collected for each sample. Results were analyzed with Kaluza v1.3 Flow Analysis Software (Beckman Coulter, Indianapolis, USA).

Vasculogenesis assays

Vasculogenesis was analyzed in Matrigel (CORNING 354234) as previously described [34]. A total of 1×10^5 HUVEC/well were seeded in a 12 well plate and either left alone or treated with ARPE-19 cells exosomes (333.3 μg of exosome protein/well) for 5 hours. The Matrigel was diluted with FBS free DMEM/F12 and was allowed to solidify for 30 min at 37°C. Images were taken with an Olympus CKX41 inverted microscope (Olympus, Tokyo, Japan), and recorded by an Olympus SC20 (Olympus) camera. Five random images/well were taken and analyzed with Image Pro-Plus Software V.6 (Media Cybernetics, Rockville, MD, USA).

Statistical analysis

The results of each experiment are presented as the mean ± S.E.M. of three treatments, repeated in triplicate. Statistical significance was determined using an ANOVA followed by Bonferroni's test with GraphPad Prism 6 software. For immunocytochemistry, the mean ± S.E.M. of the percentages was calculated and is expressed in a graphical format.

Acknowledgments

This work was partially supported by the UCV funds for research 2017-128001 and the PROMETEO grant 94/2016 from Generalitat Valenciana. Italian MIUR also supported this study, with the PRIN fund. The authors thank prof. Paolo Grieco for supplying the PG-901 compound; prof. Stephen Getting and prof. Claudio Bucolo for correcting the English.

Disclosure statement

No potential conflict of interest was reported by the authors.

Funding

This work was partially supported by grant PROMETEO #94/2016 from Generalitat Valenciana, Valencia, Spain.

ORCID

Javier Sancho-Pellúz http://orcid.org/0000-0001-5409-5760
Jorge Miguel Barcia http://orcid.org/0000-0002-3660-7977
Francisco Javier Romero http://orcid.org/0000-0001-8701-5907

References

[1] Novoselova TV, Chan LF, Clark AJL. Pathophysiology of melanocortin receptors and their accessory proteins. Best Pract Res Clin Endocrinol Metab. 2018;32:93–106.
[2] Atienzar-Aroca S, Flores-Bellver M, Serrano-Heras G, et al. Oxidative stress in retinal pigment epithelium cells increases exosome secretion and promotes angiogenesis in endothelial cells. JCell Mol Med. 2016;20: 1457–1466.
[3] Rossi S, Maisto R, Gesualdo C, et al. Activation of melanocortin receptors MC1 and MC5 attenuates retinal damage in experimental diabetic retinopathy. Med Inflammation. 2016; 2016:7368389.
[4] Maisto R, Gesualdo C, Trotta MC, et al. Melanocortin receptor agonist MCR1-5 protect photoreceptors from high-glucose damage and restore antioxidant enzymes in primary retinal cell culture. J Cell Mol Med. 2017;21:968–974.
[5] Tokarz A, Szuścik I, Kuśnierz-Cabala B, et al. Extracellular vesicles participate in the transport of cytokines and angiogenic factors in diabetic patients with ocular complications. Folia Med Cracov. 2015;4:35–48.
[6] Strauss O. The retinal pigment epithelium in visual function. Physiol Rev. 2005;85:845–888.
[7] van der Pol E, Böing AN, Harrison P, et al. Classification, functions, and clinical relevance of extracellular vesicles. Pharmacol Rev. 2012;64:676–705.
[8] Keller S, Sanderson MP, Stoeck A, et al. Exosomes: from biogenesis and secretion to biological function. Immunol Lett. 2006;107:102–108.
[9] Dhondt B, Van Deun J, Vermaerke S, et al. Urinary extracellular vesicle biomarkers in urological cancers: from discovery towards clinical implementation. Int J Biochem Cell Biol. 2018;99:236–256.
[10] Dhondt B, Rousseau Q, De Wever O, et al. Function of extracellular vesicle-associated miRNAs in metastasis. Cell Tissue Res. 2016;365:621–641.
[11] Park JE, Tan HS, Datta A, et al. Hypoxic tumor cell modulates its microenvironment to enhance angiogenic and metastatic potential by secretion of proteins and exosomes. Mol Cell Proteomics. 2010;9:1085–1099.
[12] Behl T, Kaur I, Kotwani A. Implication of oxidative stress in progression of diabetic retinopathy. Surv Ophtalmol. 2016;61:187–196.
[13] Lupo G, Motta C, Giurdanella G, et al. Role of phospholipases A2 in diabetic retinopathy: in vitro and in vivo studies. Biochem Pharmacol. 2013;86:1603–1613.
[14] Bucolo C, Drago F, Lin LR, et al. Sigma receptor ligands protect human retinal cells against oxidative stress. Neuroreport. 2006;27:17:287–291.
[15] Maugeri A, Barchitta M, Mazzone MG, et al. Resveratrol modulates SIRT1 and DNMT functions and restores LINE-1 methylation levels in ARPE-19 cells under oxidative stress and inflammation. Int J Mol Sci. 2018;20:19.
[16] Nita M, Grzybowski A. The Role of the reactive oxygen species and oxidative stress in the pathomechanism of the age-related ocular diseases and other pathologies of the anterior and posterior eye segments in adults. Oxid Med Cell Longev. 2016;2016:3164734.
[17] Beatty S, Koh H, Phil M, et al. The role of oxidative stress in the pathogenesis of age-related macular degeneration. Surv Ophthalmol. 2000;45:115–134.
[18] Winkler BS, Boulton ME, Gottsch JD, et al. Oxidative damage and age-related macular degeneration. Mol Vis. 1999;5:32.
[19] Pittalà V, Fidilio A, Lazzara F, et al. Effects of novel nitric oxide-releasing molecules against oxidative stress on retinal pigmented epithelial cells. Oxid Med Cell Longev. 2017;2017:1420892.
[20] Mettu PS, Wielgus AR, Ong SS, et al. Retinal pigment epithelium response to oxidant injury in the pathogenesis of early age-related macular degeneration. Mol Aspects Med. 2012;33:376–398.
[21] Sobrino A, Oviedo PJ, Novella S, et al. Estradiol selectively stimulates endothelial prostacyclin production through estrogen receptor-{alpha}. J Mol Edocrinol. 2010;44:237–246.
[22] Ucuzian AA, Gassman AA, East AT, et al. Molecular mediators of angiogenesis. J Burn Care Res. 2010;31:158–175.
[23] Biasutto L, Chiechi A, Couch R, et al. Retinal pigment epithelium (RPE) exosomes contain signaling phosphoproteins affected by oxidative stress. Exp Cell Res. 2013;319:2113–2123.
[24] Geminard C, Nault F, Johnstone RM, et al. Characteristics of the interaction between Hsc70 and the transferring receptor in exosomes released during reticulocyte maturation. J Biol Chem. 2001;276:9910–9916.
[25] Janowska-Wieczorek A, Wysoczynski M, Kijowski J, et al. Microvesicles derived from activated platelets induce metastasis and angiogenesis in lung cancer. Int J Cancer. 2005;113:752–760.
[26] Taieb J, Chaput N, Zitvogel L. Dendritic cellderived exosomes as cell-free peptide-based vaccines. Crit Rev Immunol. 2005;25:215–223.
[27] Villa I, Skokos D, Tkaczyk C, et al. Capacity of mouse mast cells to prime T cells and to induce specific antibody responses in vivo. Immunology. 2001;102:165–217.
[28] Enriori PJ, Chen W, Garcia-Rudaz MC, et al. α-Melanocyte stimulating hormone promotes muscle

glucose uptake via melanocortin 5 receptors. Mol Metab. 2016;5:807–822.

[29] Liu G, Li M, Saeed M, et al. αMSH inhibits adipose inflammation via reducing FoxOs transcription and blocking Akt/JNK pathway in mice. Oncotarget. 2017;8:47642–47654.

[30] Valli-Jaakola K, Suviolahti E, Schalin-Jantti C, et al. Further evidence for The role of ENPP1 in obesity: association with morbid obesity in Finns. Obesity . 2008;16 :2113–2119.

[31] Zordoky BN, El-Kadi AO. Role of NF-kappaB in the regulation of cytochrome P450 enzymes. Curr Drug Metab. 2009;10:164–178.

[32] Grieco P, Han G, Weinberg D, et al. Design and synthesis of highly potent and selective melanotropin analogues of SHU9119 modified at position 6. Biochem Biophys Res Commun. 2002;292:1075–1080.

[33] Grieco P, Cai M, Liu L, et al. Design and microwave-assisted synthesis of novel macrocyclic peptides active at melanocortin receptors: discovery of potent and selective hMC5R receptor antagonists. J Med Chem. 2008;51:2701–2707.

[34] Novella S, Lázaro-Franco M, Pérez-Cremades D. An affordable method to obtain cultured endothelial cells from peripheral blood. J Cell Mol Med. 2013;17:1475–1483.